

000 EXPLORE DATA LEFT BEHIND IN REINFORCEMENT 001 LEARNING FOR REASONING LANGUAGE MODELS 002

003 **Anonymous authors**
004

005 Paper under double-blind review
006

007 ABSTRACT 008

009 Reinforcement Learning with Verifiable Rewards (RLVR) has emerged as an ef-
010 fective approach for improving the reasoning abilities of large language mod-
011 eels (LLMs). The Group Relative Policy Optimization (GRPO) family has
012 demonstrated strong performance in training LLMs with RLVR. However, as
013 models train longer and scale larger, more training prompts become residual
014 prompts—those with zero-variance rewards that provide no training signal. Con-
015 sequently, fewer prompts contribute to training, reducing diversity and hindering
016 effectiveness. To fully exploit these residual prompts, we propose the **Explore**
017 **Residual Prompts in Policy Optimization** (ERPO) framework, which encourages
018 exploration on residual prompts and reactivates their training signals. ERPO main-
019 tains a history tracker for each prompt and adaptively increases the sampling tem-
020 perature for residual prompts that previously produced all-correct responses. This
021 encourages the model to generate more diverse reasoning traces, introducing in-
022 correct responses that revive training signals. Empirical results on the Qwen2.5
023 series demonstrate that ERPO consistently surpasses strong baselines across mul-
024 tiple mathematical reasoning benchmarks.
025

026 1 INTRODUCTION 027

028 Large language models (LLMs) have become the foundation of modern artificial intelligence, ex-
029 hibiting strong performance across domains such as mathematics, programming, and scientific prob-
030 lem solving (Team et al., 2023; Guo et al., 2025; Yang et al., 2025a). A central factor behind these
031 advancements is their capacity for extended reasoning, where models construct coherent, multi-step
032 chains of thought to address complex tasks (Wei et al., 2022; Yao et al., 2023; Muennighoff et al.,
033 2025). Reinforcement learning (RL) has emerged as a key paradigm for strengthening this capabili-
034 ty, enabling LLMs to refine their responses through interaction-driven feedback and alignment with
035 verifiable signals or human preferences (Schulman et al., 2017; Ouyang et al., 2022; Rafailov et al.,
036 2023). In particular, reinforcement learning with verifiable rewards (RLVR) has proven especially
037 effective, as it leverages tasks with automatically checkable outcomes to provide reliable supervision
038 for scaling reasoning abilities (Shao et al., 2024; Guo et al., 2025; Yang et al., 2025a).
039

040 Among recent advances in reinforcement learning for LLMs, Group Relative Policy Optimization
041 (GRPO) has emerged as a widely adopted RLVR framework (Shao et al., 2024; Guo et al., 2025).
042 Building on this foundation, subsequent research has sought to address key issues of GRPO, includ-
043 ing entropy collapse, reward noise, and training instability (Yu et al., 2025; Cui et al., 2025; Zheng
044 et al., 2025a). Furthermore, as an on-policy algorithm, GRPO has motivated efforts to develop more
045 effective sampling strategies beyond basic random decoding (Xu et al., 2025; Zheng et al., 2025c;
046 Hou et al., 2025).

047 In this work, we identify a limitation shared by the GRPO family of algorithms: as training steps and
048 model size increase, more training prompts become residual prompts that no longer provide training
049 signals yet still contain valuable information that can benefit model performance. Residual prompts
050 are those that initially provide effective training signals at the beginning of training but eventually
051 provide zero training signal or are filtered out by the RL algorithms as the well-trained policy gener-
052 ates all-correct responses for them. This reduces training diversity over time and ultimately hinders
053 further improvement through RL. Furthermore, residual prompts retain learning potential that can
be leveraged to further improve model performance, as they help the model retain acquired abilities

054
 055 Table 1: Proportion of prompts with all-correct responses under different sampling temperatures
 056 and model scales. The proportion increases with RL training process and larger model sizes, leaving
 057 more residual prompts, thereby reducing diversity and wasting valuable training signals.

	$T = 1.0$	$T = 1.1$	$T = 1.2$
Qwen2.5-3B	0%	–	–
Qwen2.5-3B + DAPO	8.7%	6.2%	2.8%
Qwen2.5-7B	0%	–	–
Qwen2.5-7B + DAPO	21.3%	15.5%	5.5%
Qwen2.5-32B	0%	–	–
Qwen2.5-32B + DAPO	74.8%	62.1	34.8%

068 and may yield novel reasoning traces. Moreover, residual prompts are not necessarily robust—small
 069 perturbations, such as increasing the sampling temperature, can easily induce errors. Table 1 reports
 070 the proportion of residual prompts with all-correct responses in the training data under different
 071 sampling temperatures and model scales.

072 To better exploit the residual prompts left behind during training, we propose the **Explore Residual**
 073 **Prompts in Policy Optimization** (ERPO) framework. ERPO introduces a novel sampling strategy
 074 that maintains a history tracker for each prompt and adaptively increases the sampling temperature
 075 for residual prompts that have previously produced all-correct responses. Specifically, ERPO records
 076 how many times a model generates all-correct responses for each prompt, and the sampling tem-
 077 perature is determined by this count. The more frequently a prompt yields all-correct responses, the
 078 higher the sampling temperature assigned to it, thereby encouraging greater exploration. As shown
 079 in Table 1, increasing the sampling temperature enables the model to explore more diverse reason-
 080 ing traces and generate incorrect responses, which reactivates the training signal and alleviates the
 081 collapse of prompt diversity.

082 Overall, **our contributions** can be summarized as follows:

- 083 • We identify a key limitation of the GRPO family: residual prompts accumulate as training
 084 progresses and models scale, leading to reduced training diversity and the loss of valuable
 085 training signals from residual prompts.
- 086 • We propose the ERPO framework, which encourages models to adaptively explore residual
 087 data and recover their learning potential. ERPO maintains a history tracker for each prompt and
 088 adaptively increases the sampling temperature for residual prompts.
- 089 • Extensive experiments on several math reasoning benchmarks demonstrate the effectiveness of
 090 ERPO in both average and majority-vote evaluations, with particularly strong improvements on
 091 data that are likely not contaminated, such as AIME2025.

094 2 RELATED WORK

096 **Reinforcement learning for LLM reasoning.** Reinforcement learning (RL) has become a central
 097 approach for enhancing the reasoning abilities of large language models (LLMs) in domains such
 098 as mathematics, programming, and problem solving (Dubey et al., 2024; Zhou et al., 2025). Early
 099 general-purpose algorithms like Proximal Policy Optimization (PPO) provided a practical frame-
 100 work for fine-tuning LLMs through sampled rollouts and reward feedback (Schulman et al., 2015;
 101 2017). More recently, RLVR methods such as Group Relative Policy Optimization (GRPO) have
 102 emerged as effective alternatives to PPO, removing the critic model while maintaining strong per-
 103 formance on reasoning benchmarks (Guo et al., 2025; Shao et al., 2024). Several extensions have been
 104 proposed to address the limitations of GRPO: Cui et al. (2025); Wang et al. (2025); Cheng et al.
 105 (2025); Zheng et al. (2025c) mitigates the entropy collapse problem during training; Zheng et al.
 106 (2025a); Yang et al. (2025b) aims to stabilize the optimization process, and DAPO (Yu et al., 2025)
 107 tackles both issues while filtering noisy rewards for training data. However, all these methods obtain
 108 no training signal from residual prompts, thereby missing valuable information during training. To

108 address this limitation, ERPO reactivates the training signal of residual prompts and learns useful
 109 information from them.
 110

111 **Data Sampling Strategies.** The outputs of LLMs rely heavily on data sampling strategies to balance
 112 diversity and quality. Common strategies include greedy search, beam search, and various random
 113 sampling techniques such as top-k and top-p (Zhao et al., 2023; Minaee et al., 2024). In RLVR,
 114 the model generates on-policy responses and assigns them verifiable rewards during training. Basic
 115 random decoding is widely used in RLVR algorithms such as GRPO and DAPO (Guo et al., 2025;
 116 Yu et al., 2025). Beyond this, several works explore alternative sampling strategies. Hou et al. (2025)
 117 leverages tree search to find correct responses with higher probability. Zheng et al. (2025c) forks
 118 responses at high-entropy tokens. Shrivastava et al. (2025) dynamically allocates additional training
 119 resources to harder problems based on real-time difficulty estimates. Xu et al. (2025) selects a subset
 120 of responses to maximize reward variation. Zheng et al. (2025b) predicts and skips uninformative
 121 prompts using reward training dynamics. Zhang et al. (2025) progressively exposes the model to
 122 increasingly challenging samples. Nevertheless, none of these methods are specifically designed to
 123 leverage information from residual prompts.

124 3 PRELIMINARIES

126 **Notation** We define an autoregressive language model parameterized by θ as a policy π_θ . Let q
 127 denote a query and \mathcal{D} the query set. For a response o to query q , its likelihood under π_θ is expressed
 128 as

$$129 \pi_\theta(o \mid q) = \prod_{t=1}^{|o|} \pi_\theta(o_{i,t} \mid q, o_{i,<t}), \quad (1)$$

132 where $|o|$ is the number of tokens in o .

133 **Group Relative Policy Optimization (GRPO)** (Shao et al., 2024; Guo et al., 2025) has shown
 134 strong effectiveness for fine-tuning LLMs. Unlike traditional approaches that rely on a critic network
 135 of comparable size to the policy, GRPO estimates the baseline directly from group-level rewards.
 136 For a specific question-answer pair (q, a) , the behavior policy $\pi_{\theta_{\text{old}}}$ samples a group of G individual
 137 responses $\{o_i\}_{i=1}^G$. Then, the advantage of the i -th response is calculated by normalizing the group-
 138 level rewards $\{R_i\}_{i=1}^G$:

$$139 \hat{A}_{i,t} = \frac{r_i - \text{mean}(\{R_i\}_{i=1}^G)}{\text{std}(\{R_i\}_{i=1}^G)}. \quad (2)$$

141 Building on the group-normalized advantages, GRPO optimizes the policy with a clipped objective
 142 that stabilizes updates and a KL regularization term that constrains divergence from the reference
 143 model. The objective is defined as:

$$145 \mathcal{J}_{\text{GRPO}}(\theta) = \mathbb{E}_{(q,a) \sim \mathcal{D}, \{o_i\}_{i=1}^G \sim \pi_{\theta_{\text{old}}}(\cdot \mid q)} \left[\begin{aligned} & \frac{1}{G} \sum_{i=1}^G \frac{1}{|o_i|} \sum_{t=1}^{|o_i|} \left(\min \left(r_{i,t}(\theta) \hat{A}_{i,t}, \text{clip} \left(r_{i,t}(\theta), 1 - \varepsilon, 1 + \varepsilon \right) \hat{A}_{i,t} \right) \right. \\ & \left. - \beta D_{\text{KL}}(\pi_\theta \parallel \pi_{\text{ref}}) \right) \end{aligned} \right], \quad (3)$$

152 where $r_{i,t}(\theta)$ is the importance ratio between the old and new policy:

$$154 r_{i,t}(\theta) = \frac{\pi_\theta(o_{i,t} \mid q, o_{i,<t})}{\pi_{\theta_{\text{old}}}(o_{i,t} \mid q, o_{i,<t})}. \quad (4)$$

157 **Decoupled Clip and Dynamic Sampling Policy Optimization (DAPO)** (Yu et al., 2025) introduces
 158 four key improvements: Clip-Higher promotes output diversity and mitigates entropy col-
 159 lapsed; Dynamic Sampling is designed to enhance training efficiency and stability; Token-Level Pol-
 160 icy Gradient Loss plays a critical role in handling long chain-of-thought reasoning; and Overlong
 161 Reward Shaping reduces reward noise while stabilizing optimization. Building on these compo-
 162 nents, DAPO optimizes the policy with the following objective:

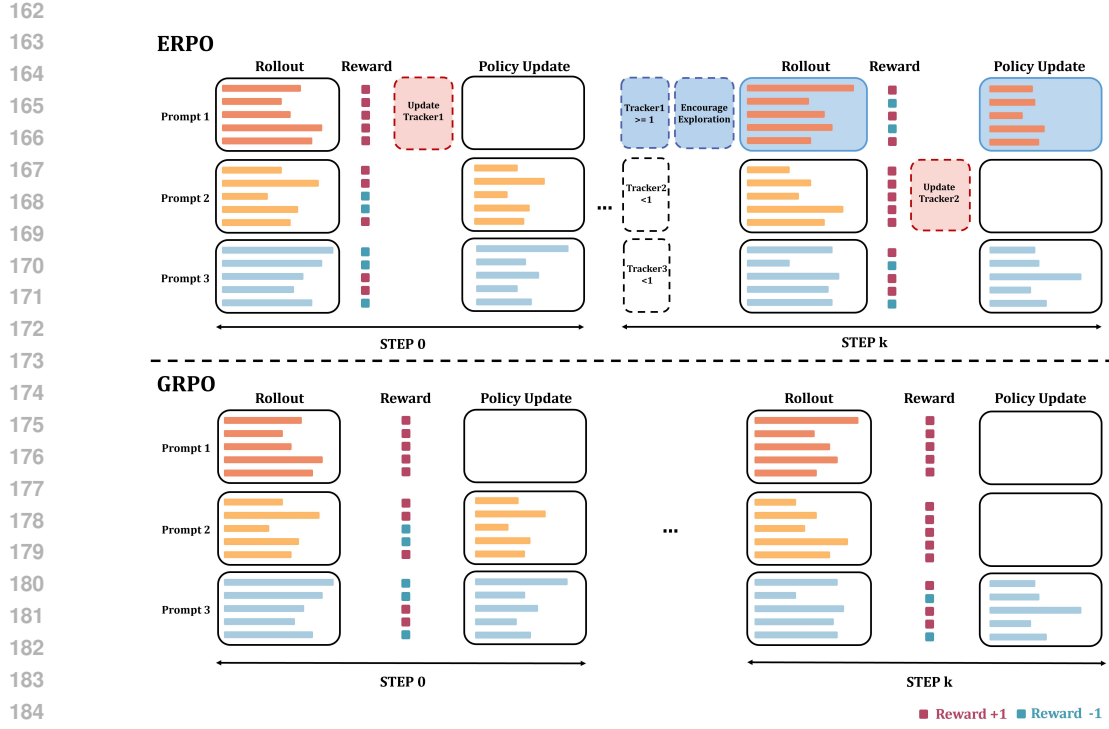


Figure 1: Comparison between ERPO and GRPO. During RL training, the policy gradually learns from the training data, resulting in more residual prompts with all-correct responses. In GRPO, residual prompts yield zero-variance rewards and thus provide no training signal for policy updates, reducing the effectiveness of training data. In contrast, ERPO maintains a tracker for each prompt to record the number of times it produces all-correct responses, and adaptively encourages exploration on residual prompts to trigger incorrect responses and reactivate the training signal.

$$\begin{aligned}
 \mathcal{J}_{\text{DAPO}}(\theta) = & \mathbb{E}_{(q, a) \sim \mathcal{D}, \{o_i\}_{i=1}^G \sim \pi_{\theta_{\text{old}}}(\cdot | q)} \\
 & \left[\frac{1}{\sum_{i=1}^G |o_i|} \sum_{i=1}^G \sum_{t=1}^{|o_i|} \min \left(r_{i,t}(\theta) \hat{A}_{i,t}, \text{clip} \left(r_{i,t}(\theta), 1 - \varepsilon_{\text{low}}, 1 + \varepsilon_{\text{high}} \right) \hat{A}_{i,t} \right) \right] \quad (5) \\
 \text{s.t. } & 0 < \left| \{o_i \mid \text{is_equivalent}(a, o_i)\} \right| < G,
 \end{aligned}$$

where a is the ground-truth answer of query q .

4 METHODOLOGY

ERPO is proposed to leverage the training information contained in residual prompts to improve reinforcement learning for reasoning language models. Section 4.1 introduces the idea of reactivating the training signal from residual prompts that are otherwise discarded during RL training. Section 4.2 describes how ERPO predicts whether a prompt is residual and adaptively modifies the sampling strategy. It further explains how ERPO adjusts the sampling temperature to encourage different levels of exploration based on a history tracker.

4.1 REACTIVATE TRAINING SIGNAL

Current RLRV algorithms usually discard residual prompts that contain all-correct responses by assigning them zero advantage (Guo et al., 2025) or by directly filtering them out from the training batch (Yu et al., 2025). Consequently, available training prompts continually decreases with ongoing

216 RL training and increasing model size, leading to a gradual reduction in both the size and diversity of
 217 the training dataset. As shown in Table 1, larger models with longer training generally produce more
 218 residual prompts that yield all-correct responses. Furthermore, as training progresses and the policy
 219 evolves, new reasoning traces and directions may be generated for the residual prompts, which can
 220 help the model learn more diverse reasoning patterns. In addition, training on residual prompts can
 221 reinforce the reasoning abilities the model has already acquired.

222 To leverage the training signal from residual prompts that are left behind by current RL algorithms,
 223 we propose a simple method to reactivate them. For residual prompts with all-correct responses, we
 224 replace the zero advantage with a small positive advantage by introducing a pseudo-negative reward
 225 into the advantage computation. The new Reactivated Advantage (RA) for prompts with all-correct
 226 responses is:

$$\hat{RA}_{i,t} = \frac{r_i - \text{mean}(\{R_i^+\}_{i=1}^G \cup \{R^-\})}{\text{std}(\{R_i^+\}_{i=1}^G \cup \{R^-\})}. \quad (6)$$

227 where R^+ is the reward for correct responses and R^- is the reward for incorrect responses. Using
 228 RA, residual prompts with all-correct responses still retain a small positive advantage, providing a
 229 valid training signal instead of being discarded by the RL algorithm.

233 4.2 EXPLORE RESIDUAL PROMPTS IN POLICY OPTIMIZATION

235 Although using the reactivated advantage can force the model to learn information from residual
 236 prompts, residual prompts will dominate the training along the training process and model scales up,
 237 leaving less negative feedback and impede the training effectiveness. (Chen et al., 2025). Furthermore,
 238 the model may suffer from an imbalance between exploration and exploitation, restricting
 239 exploration to a narrow search space and potentially causing overfitting on all-correct prompts, par-
 240 ticularly at larger model scales. (Xiong et al., 2025)

241 To address this limitation, we propose to adaptively encourage exploration on residual prompts
 242 by controlling their sampling temperature. As shown in Table 1, a higher sampling temperature
 243 can trigger incorrect responses, thereby reactivating the training signals of residual prompts. Note
 244 that training data typically exhibit strong temporal correlations across epochs (Zheng et al., 2022),
 245 meaning that a prompt producing all-correct responses in the current epoch is likely to do so again
 246 in the following epoch (Zheng et al., 2025b). Thus, we can maintain a history tracker H_i to track
 247 how many times the policy generates all-correct responses for a prompt q_i :

$$H_i^{(0)} = 0, \quad H_i^{(t)} = H_i^{(t-1)} + \mathbf{1}_{q_i \text{ has all-correct responses at step } t} \quad (7)$$

248 Then H_i is used to determine whether we should assign a larger sampling temperature to prompt q_i .
 249 If H_i is greater than 0, it means that prompt q_i is already easy for the policy to generate all-correct
 250 responses, and it is very likely to provide no training signals the next time the policy samples it.
 251 Therefore, we assign a larger sampling temperature to prompts with $H_i > 0$ to encourage more
 252 exploration of their reasoning traces and to reactivate the training signal by triggering incorrect
 253 responses.

254 Since the robustness of prompts varies, some residual prompts require only a marginal increase in
 255 sampling temperature to induce incorrect responses, whereas others necessitate substantially larger
 256 adjustments. At the same time, it is essential to preserve the benefits of on-policy learning by con-
 257 straining distributional shifts within a reasonable range to ensure stable and effective training. As-
 258 signing excessively large sampling temperatures is particularly detrimental for prompts with lower
 259 robustness. This trade-off highlights the difficulty of selecting a single, unified sampling temperature
 260 that can consistently induce incorrect responses, enhance exploration, and maintain a manageable
 261 distribution shift across all residual prompts. Therefore, ERPO introduces a prompt-adaptive adjust-
 262 ment of the sampling temperature:

$$T_i^{(t)} = \min(T_0 + T_s \cdot H_i^{(t)}, T_{max}) \quad (8)$$

263 where T_0 , T_{max} , and T_s are hyperparameters representing the initial temperature, maximum temper-
 264 ature, and temperature step size, respectively. In this way, ERPO gradually increases the sampling
 265 temperature of residual prompts until the policy generates incorrect responses. This enables ERPO
 266 to strike a balance between reactivating training signals, encouraging exploration, and maintaining
 267 a reasonable distribution shift. In general, our ERPO framework can be summarized in Algorithm 1:

270 **Algorithm 1** ERPO framework271 **Input:** Policy π_θ , reward model R ,272 Prompt set $\mathcal{D} = \{q_i\}_{i=1}^N$, history tracker $\{H_i\}_{i=1}^N$ (init. $H_i^{(0)} = 0$),
273 Rollouts per prompt n , temperatures (T_0, T_{\max}) , step size T_s , steps K 274 **Output:** Updated policy $\pi_{\theta_{\text{updated}}}$

 275 1: **for** $t = 1, 2, \dots, K$ **do**
 276 2: Sample a mini-batch $\mathbf{q} \subseteq \mathcal{D}$
 277 3: **for** each $q_i \in \mathbf{q}$ **do**
 278 4: $T_i^{(t)} \leftarrow \min(T_0 + T_s \cdot H_i^{(t-1)}, T_{\max})$
 279 5: Sample n rollouts $\mathbf{o}_i = (o_1, \dots, o_n)$ for q_i using π_θ at temperature $T_i^{(t)}$
 280 6: Compute rewards $\mathbf{r}_i = (r_1, \dots, r_n)$ with R ; $\mathbf{acc} \leftarrow \mathbf{1}_{\text{all } o_j \text{ correct}}$
 281 7: $H_i^{(t)} \leftarrow H_i^{(t-1)} + \mathbf{1}_{\mathbf{acc}=1}$
 282 8: **end for**
 283 9: Update π_θ using an RL algorithm with data $\mathcal{B} = \{(\mathbf{q}, \mathbf{o}, \mathbf{r})\}$
 284 10: **end for**
 285 11: **return** $\pi_{\theta_{\text{updated}}} \leftarrow \pi_\theta$

288 **5 EXPERIMENTS**291 In this section, we first outline the implementation details, including training details and evalua-
292 tion. We then present the main results, comparing ERPO against baseline approaches across several
293 math reasoning benchmarks. Finally, we provide additional experimental results to support further
294 analysis.295 **5.1 IMPLEMENTATION DETAILS**297 **Training details:** Following recent studies (Zheng et al., 2025c; Cheng et al., 2025; Shao et al.,
298 2025) that apply RLVR to train LMMs for math reasoning tasks, we adopt Qwen2.5-3B and
299 Qwen2.5-7B (Qwen et al., 2025) as our backbone models. Consistent with prior work (Yu et al.,
300 2025; Cheng et al., 2025; Cui et al., 2025), we use the DAPO-Math-17K dataset (Yu et al., 2025)
301 for training. To achieve strong performance, we adopt the DAPO algorithm (Yu et al., 2025). Prior
302 works (Yu et al., 2025; Cheng et al., 2025) has demonstrated its superior effectiveness and stability
303 over vanilla GRPO, and we employ it both as the baseline and as the optimization method for ERPO.
304 The learning rate is set to 1×10^{-6} with a linear warm-up over 10 rollout steps. For rollout, we
305 use a prompt batch size of 512, sampling 16 responses per prompt. During training, the mini-batch
306 size is set to 512, resulting in 16 gradient updates per rollout step. The initial rollout temperature
307 T_0 is set to 1.0. The temperature increment step T_s is set to 0.02 for Qwen2.5-3B and 0.05 for
308 Qwen2.5-7B, while the maximum rollout temperature T_{\max} is set to 1.2 for Qwen2.5-3B and 1.4
309 for Qwen2.5-7B, respectively. Rewards are assigned as 1 for correct responses and -1 otherwise.
310 All experiments are conducted using the verl framework (Sheng et al., 2024). More details can be
311 found in the Appendix.312 **Evaluation:** We evaluate our models on AIME 2025/2024, AMC 2023, and MATH500 (Hendrycks
313 et al., 2021), using a rollout temperature of 1.0 and top- p sampling with $p = 0.7$. For AIME and
314 AMC, we sample $K = 32$ independent responses for each prompt and report the average accuracy
315 as $\text{mean}@K$. In addition, we provide the majority-vote (Zhao et al., 2023) accuracy $\text{maj}@K$
316 and $\text{pass}@K$ (Cheng et al., 2025) as complementary metrics. For the larger and less challenging
317 MATH500 benchmark, we sample $K = 4$ responses per prompt and report the $\text{mean}@4$, $\text{maj}@4$
318 and $\text{pass}@4$ metrics. All evaluations are conducted using the verl framework (Sheng et al., 2024)
319 and follow the same evaluation protocol as DAPO (Yu et al., 2025). More details can be found in
320 the Appendix.321 **5.2 BENCHMARK COMPARISONS**322 In this section, we compare the performance of DAPO, Reactivated Advantage (RA), and ERPO
323 on the AIME25, AIME24, AMC23, and MATH500 benchmarks. The detailed results are shown

324
 325 Table 2: Performance comparison of the Qwen2.5-3B and Qwen2.5-7B models trained with DAPO,
 326 +RA, and +ERPO. Evaluations use mean@32, maj@32, and pass@32 for AIME25, AIME24, and
 327 AMC23; MATH500 is reported with mean@4, maj@4, and pass@4. The Avg. columns average the
 328 mean, maj, and pass across datasets.

Method	AIME25			AIME24			AMC23			MATH500			Avg.		
	mean@32	maj@32	pass@32	mean@32	maj@32	pass@32	mean@32	maj@32	pass@32	mean@4	maj@4	pass@4	mean	maj	pass
Qwen2.5-3B															
DAPO	4.5	8.9	23.3	9.5	15.2	26.7	58.4	68.0	85.0	59.8	61.7	75.4	33.0	38.5	52.6
+RA	7.7	11.4	30.0	9.6	14.1	30.0	59.1	67.1	85.0	55.0	57.7	76.4	32.9	37.6	55.4
+ERPO	5.5	8.8	30.0	10.3	16.0	36.7	60.8	70.0	90.0	59.5	62.3	77.6	34.0	39.3	58.6
Qwen2.5-7B															
DAPO	12.6	16.9	33.3	17.5	20.1	33.3	76.7	81.4	87.5	75.5	76.2	83.2	45.6	48.7	59.3
+RA	13.5	16.4	30.0	16.1	18.1	36.7	75.8	80.2	87.5	76.1	76.7	83.4	45.4	47.9	59.4
+ERPO	14.2	19.4	36.7	19.0	21.2	43.3	76.4	81.5	92.5	75.8	76.6	84.4	46.4	49.7	64.2

337
 338
 339 In Table 2. On Qwen-3B, both RA and ERPO achieve higher mean and majority-vote accuracy
 340 than the baseline DAPO. The improvement of RA demonstrates that residual prompts still contain
 341 valuable training information and should not be totally excluded from RL training. On AIME2025,
 342 RA achieves a remarkable performance gain compared to the baseline: around a 70% improvement
 343 on *mean*@32 and a 28% improvement on *maj*@32. Since AIME2025 is shown to suffer less from
 344 data contamination during model pretraining than the other math benchmarks (Wu et al., 2025),
 345 these results confirm that learning on residual prompts is particularly helpful for tasks that are novel
 346 and challenging for the model.

347 On Qwen2.5-7B, ERPO achieves the best overall performance in both mean and majority-vote accuracy
 348 compared to DAPO and RA, indicating the scalability of our algorithm. On AIME2025, ERPO
 349 achieves the largest improvement over the baseline, with an increase of approximately 12% and 16%
 350 on *mean*@32 and *maj*@32. However, unlike the results on the 3B model, RA performs worse than
 351 ERPO. A possible reason is that reactivating all residual prompts may lead to overfitting when the
 352 proportion of residual prompts is high during training. As shown in Table 1, Qwen2.5-7B has more
 353 than 20% residual prompts, making this issue more pronounced as the model scales up. In contrast,
 354 ERPO avoids this problem by setting T_{\max} , which prevents unbounded increases in sampling temperature.
 355 Once a residual prompt is fully learned and robust to higher temperatures, it no longer
 356 provides a training signal.

357 In summary, RA verifies that residual prompts contain information that can still benefit model training
 358 and should not be totally discarded. ERPO further provides an effective sampling strategy that
 359 leverages training signals from residual prompts and scales effectively to larger models.

360 5.3 EXPLORATION ON RESIDUAL PROMPTS

362 To investigate the effect of sampling temperature on residual prompts, we conduct experiments
 363 to measure the proportion of residual prompts under different temperature settings. Specifically,
 364 we select a 2k subset from our training dataset DAPO-Math-17K, sample each prompt 16 times
 365 following the same training configuration, and calculate the proportion of residual prompts within
 366 this subset. We evaluate Qwen2.5-3B, Qwen2.5-7B, and Qwen2.5-32B trained with DAPO. For
 367 Qwen2.5-32B+DAPO, we use the publicly released checkpoints from DAPO (Yu et al., 2025). The
 368 detailed results are presented in Table 1. Our findings highlight three key observations: (1) the
 369 proportion of residual prompts increases after training; (2) larger models tend to produce more
 370 residual prompts, revealing the challenge of scaling RLVR with model size; and (3) higher sampling
 371 temperatures encourage greater exploration and can elicit more incorrect responses from residual
 372 prompts.

373 On the other hand, we also examine the effect of sampling temperature on prompts with all-incorrect
 374 responses. The experimental settings are kept the same, and the results are presented in Table 3. The
 375 findings indicate that RL training and model scaling reduce the proportion of prompts with all-
 376 incorrect responses. Moreover, sampling temperature has a much smaller impact on this proportion
 377 than on residual prompts. Therefore, ERPO is applied only to residual prompts that are more likely
 378 to yield all-correct responses.

378

379
Table 3: Proportion of prompts with **all-incorrect** responses under different sampling temperatures
380 and model scales.

	$T = 1.0$	$T = 1.1$	$T = 1.2$
Qwen2.5-3B	73.0%	–	–
Qwen2.5-3B + DAPO	39.6%	40.6%	44.0%
Qwen2.5-7B	68.9%	–	–
Qwen2.5-7B + DAPO	25.1%	26.9%	33.2%
Qwen2.5-32B	48.9%	–	–
Qwen2.5-32B + DAPO	7.0%	7.9%	15.2%

389

390
Table 4: Sensitivity analysis on temperature range (T_s, T_{\max}) using Qwen2.5-3B. Here, T_s denotes
391 the step size of rollout temperature and T_{\max} denotes the maximum rollout temperature reached during
392 training. Evaluations use *mean@32*, *maj@32* and *pass@32* for AIME25, AIME24, AMC23;
393 MATH500 uses *mean@4*, *maj@4* and *pass@4*. The Avg. columns average mean, maj, and pass
394 across datasets.

(T_{\max}, T_{\min})	AIME25			AIME24			AMC23			MATH500			Avg.		
	mean@32	maj@32	pass@32	mean@32	maj@32	pass@32	mean@32	maj@32	pass@32	mean@4	maj@4	pass@4	mean	maj	pass
(0.02, 1.2)	5.5	8.8	30.0	10.3	16.0	36.7	60.8	70.0	90.0	59.5	62.3	77.6	34.0	39.3	58.6
(0.05, 1.2)	5.6	9.4	26.7	8.8	14.2	30.0	59.2	69.5	87.5	57.5	60.2	73.8	32.8	38.3	54.5
(0.05, 1.4)	3.6	5.5	33.3	9.9	14.6	33.3	59.6	67.7	85.0	58.4	60.8	75.4	32.9	37.2	56.8

395

396

400
5.4 SENSITIVE ANALYSIS

401

We conduct a sensitivity analysis on the temperature increment step (T_s) and the maximum rollout temperature (T_{\max}) to evaluate their impact on the Qwen2.5-3B model. Specifically, we experiment with three parameter settings: $T_s = 0.02, T_{\max} = 1.2$; $T_s = 0.05, T_{\max} = 1.2$; and $T_s = 0.05, T_{\max} = 1.4$. The performance under these settings is reported in Table 4. The results show that $T_s = 0.02$ and $T_{\max} = 1.2$ yield the best overall performance, while increasing either T_s or T_{\max} leads to performance degradation. Nevertheless, the models still achieve comparable performance on *mean@K* and *maj@K*, and exhibit non-trivial improvements on the *pass@K* metrics. These findings suggest that models with lower task robustness require smaller temperature perturbations to maintain stable optimization.

411

412

5.5 FURTHER ANALYSIS

413

Sampling Temperature The average and maximum sampling temperatures during the ERPO training process are shown in Figure 2. The maximum temperature increases linearly, whereas the average temperature increases exponentially, indicating that more prompts become residual prompts whose sampling temperatures are raised by ERPO. Setting an upper bound on the temperature, T_{\max} , is necessary to prevent uncontrolled growth of the sampling temperature.

427

6 CONCLUSION

428

430
431

In this work, we address a key limitation of GRPO-based reinforcement learning for LLMs: the accumulation of residual prompts that diminish training diversity and leave valuable signals underutilized. To tackle this, we introduce the ERPO framework, which adaptively adjusts sampling

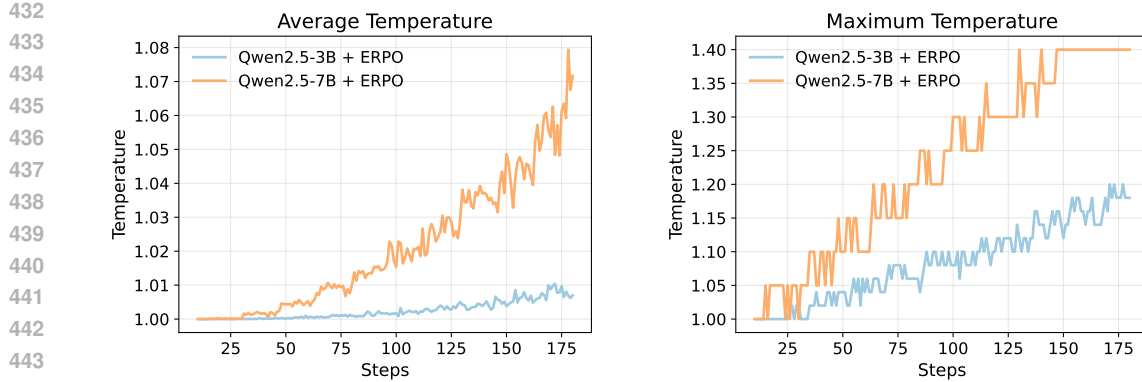


Figure 2: The average and maximum sampling temperatures during the ERPO training process. The steps shown here are the prompt generation steps.

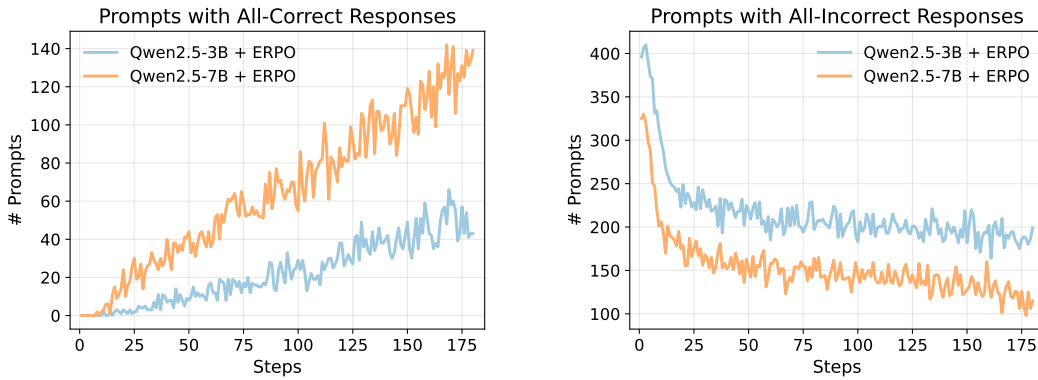


Figure 3: The number of residual prompts with all-correct responses and prompts with all-incorrect responses during the ERPO training process. The steps shown here are the prompt generation steps.

temperature based on prompt history to reactivate training signals and encourage broader exploration. Our experiments across multiple math reasoning benchmarks demonstrate that ERPO not only mitigates prompt collapse but also improves both average and majority-vote performance, with especially strong gains on tasks less affected by data contamination. These results highlight the potential of exploiting residual prompts as a promising direction for advancing reinforcement learning with verifiable rewards.

ETHICS STATEMENT

This work uses only publicly available mathematical datasets without personal or sensitive information. The study does not involve human subjects or animals. Our method focuses on improving reasoning in math tasks, with minimal risk of societal harm, and is intended solely for research purposes.

REPRODUCIBILITY STATEMENT

To facilitate reproducibility, we provide detailed implementation settings in Section 5.1 and section A in the Appendix. In addition, we release the source code in the supplementary materials, enabling readers to replicate all experiments and results reported in this paper.

486 REFERENCES
487

488 Huayu Chen, Kaiwen Zheng, Qinsheng Zhang, Ganqu Cui, Yin Cui, Haotian Ye, Tsung-Yi Lin,
489 Ming-Yu Liu, Jun Zhu, and Haoxiang Wang. Bridging supervised learning and reinforcement
490 learning in math reasoning. *arXiv preprint arXiv:2505.18116*, 2025.

491 Daixuan Cheng, Shaohan Huang, Xuekai Zhu, Bo Dai, Wayne Xin Zhao, Zhenliang Zhang, and
492 Furu Wei. Reasoning with exploration: An entropy perspective. *arXiv preprint arXiv:2506.14758*,
493 2025.

494 Ganqu Cui, Yuchen Zhang, Jiacheng Chen, Lifan Yuan, Zhi Wang, Yuxin Zuo, Haozhan Li, Yuchen
495 Fan, Huayu Chen, Weize Chen, et al. The entropy mechanism of reinforcement learning for
496 reasoning language models. *arXiv preprint arXiv:2505.22617*, 2025.

497 Abhimanyu Dubey, Abhinav Jauhri, Abhinav Pandey, Abhishek Kadian, Ahmad Al-Dahle, Aiesha
498 Letman, Akhil Mathur, Alan Schelten, Amy Yang, Angela Fan, et al. The llama 3 herd of models.
499 *arXiv e-prints*, pp. arXiv–2407, 2024.

500 Daya Guo, Dejian Yang, Haowei Zhang, Junxiao Song, Ruoyu Zhang, Runxin Xu, Qihao Zhu,
501 Shirong Ma, Peiyi Wang, Xiao Bi, et al. Deepseek-r1: Incentivizing reasoning capability in llms
502 via reinforcement learning. *arXiv preprint arXiv:2501.12948*, 2025.

503 Dan Hendrycks, Collin Burns, Saurav Kadavath, Akul Arora, Steven Basart, Eric Tang, Dawn Song,
504 and Jacob Steinhardt. Measuring mathematical problem solving with the math dataset. *arXiv
505 preprint arXiv:2103.03874*, 2021.

506 Zhenyu Hou, Ziniu Hu, Yujiang Li, Rui Lu, Jie Tang, and Yuxiao Dong. Treerl: Llm reinforcement
507 learning with on-policy tree search. *arXiv preprint arXiv:2506.11902*, 2025.

508 Shervin Minaee, Tomas Mikolov, Narjes Nikzad, Meysam Chenaghlu, Richard Socher, Xavier Am-
509 triain, and Jianfeng Gao. Large language models: A survey. *arXiv preprint arXiv:2402.06196*,
510 2024.

511 Niklas Muennighoff, Zitong Yang, Weijia Shi, Xiang Lisa Li, Li Fei-Fei, Hannaneh Hajishirzi, Luke
512 Zettlemoyer, Percy Liang, Emmanuel Candès, and Tatsunori Hashimoto. s1: Simple test-time
513 scaling. *arXiv preprint arXiv:2501.19393*, 2025.

514 Long Ouyang, Jeffrey Wu, Xu Jiang, Diogo Almeida, Carroll Wainwright, Pamela Mishkin, Chong
515 Zhang, Sandhini Agarwal, Katarina Slama, Alex Ray, et al. Training language models to fol-
516 low instructions with human feedback. *Advances in neural information processing systems*, 35:
517 27730–27744, 2022.

518 Qwen, :, An Yang, Baosong Yang, Beichen Zhang, Binyuan Hui, Bo Zheng, Bowen Yu, Chengyuan
519 Li, Dayiheng Liu, Fei Huang, Haoran Wei, Huan Lin, Jian Yang, Jianhong Tu, Jianwei Zhang,
520 Jianxin Yang, Jiaxi Yang, Jingren Zhou, Junyang Lin, Kai Dang, Keming Lu, Keqin Bao, Kexin
521 Yang, Le Yu, Mei Li, Mingfeng Xue, Pei Zhang, Qin Zhu, Rui Men, Runji Lin, Tianhao Li,
522 Tianyi Tang, Tingyu Xia, Xingzhang Ren, Xuancheng Ren, Yang Fan, Yang Su, Yichang Zhang,
523 Yu Wan, Yuqiong Liu, Zeyu Cui, Zhenru Zhang, and Zihan Qiu. Qwen2.5 technical report, 2025.
524 URL <https://arxiv.org/abs/2412.15115>.

525 Rafael Rafailov, Archit Sharma, Eric Mitchell, Christopher D Manning, Stefano Ermon, and Chelsea
526 Finn. Direct preference optimization: Your language model is secretly a reward model. *Advances
527 in neural information processing systems*, 36:53728–53741, 2023.

528 John Schulman, Sergey Levine, Pieter Abbeel, Michael Jordan, and Philipp Moritz. Trust region
529 policy optimization. In *International conference on machine learning*, pp. 1889–1897. PMLR,
530 2015.

531 John Schulman, Filip Wolski, Prafulla Dhariwal, Alec Radford, and Oleg Klimov. Proximal policy
532 optimization algorithms. *arXiv preprint arXiv:1707.06347*, 2017.

533 Rulin Shao, Shuyue Stella Li, Rui Xin, Scott Geng, Yiping Wang, Sewoong Oh, Simon Shaolei
534 Du, Nathan Lambert, Sewon Min, Ranjay Krishna, et al. Spurious rewards: Rethinking training
535 signals in rlvr. *arXiv preprint arXiv:2506.10947*, 2025.

540 Zhihong Shao, Peiyi Wang, Qihao Zhu, Runxin Xu, Junxiao Song, Xiao Bi, Haowei Zhang,
 541 Mingchuan Zhang, YK Li, Yang Wu, et al. Deepseekmath: Pushing the limits of mathemati-
 542 cal reasoning in open language models. *arXiv preprint arXiv:2402.03300*, 2024.

543 Guangming Sheng, Chi Zhang, Zilingfeng Ye, Xibin Wu, Wang Zhang, Ru Zhang, Yanghua Peng,
 544 Haibin Lin, and Chuan Wu. Hybridflow: A flexible and efficient rlhf framework. *arXiv preprint*
 545 *arXiv: 2409.19256*, 2024.

546 Vaishnavi Shrivastava, Ahmed Awadallah, Vidhisha Balachandran, Shivam Garg, Harkirat Behl,
 547 and Dimitris Papailiopoulos. Sample more to think less: Group filtered policy optimization for
 548 concise reasoning. *arXiv preprint arXiv:2508.09726*, 2025.

549 Gemini Team, Rohan Anil, Sebastian Borgeaud, Jean-Baptiste Alayrac, Jiahui Yu, Radu Soricut,
 550 Johan Schalkwyk, Andrew M Dai, Anja Hauth, Katie Millican, et al. Gemini: a family of highly
 551 capable multimodal models. *arXiv preprint arXiv:2312.11805*, 2023.

552 Shenzhi Wang, Le Yu, Chang Gao, Chujie Zheng, Shixuan Liu, Rui Lu, Kai Dang, Xionghui Chen,
 553 Jianxin Yang, Zhenru Zhang, et al. Beyond the 80/20 rule: High-entropy minority tokens drive
 554 effective reinforcement learning for llm reasoning. *arXiv preprint arXiv:2506.01939*, 2025.

555 Jason Wei, Xuezhi Wang, Dale Schuurmans, Maarten Bosma, Fei Xia, Ed Chi, Quoc V Le, Denny
 556 Zhou, et al. Chain-of-thought prompting elicits reasoning in large language models. *Advances in*
 557 *neural information processing systems*, 35:24824–24837, 2022.

558 Mingqi Wu, Zhihao Zhang, Qiaole Dong, Zhiheng Xi, Jun Zhao, Senjie Jin, Xiaoran Fan, Yuhao
 559 Zhou, Huijie Lv, Ming Zhang, et al. Reasoning or memorization? unreliable results of reinforce-
 560 ment learning due to data contamination. *arXiv preprint arXiv:2507.10532*, 2025.

561 Wei Xiong, Jiarui Yao, Yuhui Xu, Bo Pang, Lei Wang, Doyen Sahoo, Junnan Li, Nan Jiang, Tong
 562 Zhang, Caiming Xiong, et al. A minimalist approach to llm reasoning: from rejection sampling
 563 to reinforce. *arXiv preprint arXiv:2504.11343*, 2025.

564 Yixuan Even Xu, Yash Savani, Fei Fang, and Zico Kolter. Not all rollouts are useful: Down-sampling
 565 rollouts in llm reinforcement learning. *arXiv preprint arXiv:2504.13818*, 2025.

566 An Yang, Anfeng Li, Baosong Yang, Beichen Zhang, Binyuan Hui, Bo Zheng, Bowen Yu,
 567 Chang Gao, Chengan Huang, Chenxu Lv, et al. Qwen3 technical report. *arXiv preprint*
 568 *arXiv:2505.09388*, 2025a.

569 Shihui Yang, Chengfeng Dou, Peidong Guo, Kai Lu, Qiang Ju, Fei Deng, and Rihui Xin. Dcpo:
 570 Dynamic clipping policy optimization. *arXiv preprint arXiv:2509.02333*, 2025b.

571 Shunyu Yao, Dian Yu, Jeffrey Zhao, Izhak Shafran, Tom Griffiths, Yuan Cao, and Karthik
 572 Narasimhan. Tree of thoughts: Deliberate problem solving with large language models. *Ad-*
 573 *vances in neural information processing systems*, 36:11809–11822, 2023.

574 Qiying Yu, Zheng Zhang, Ruofei Zhu, Yufeng Yuan, Xiaochen Zuo, Yu Yue, Weinan Dai, Tiantian
 575 Fan, Gaohong Liu, Lingjun Liu, et al. Dapo: An open-source llm reinforcement learning system
 576 at scale. *arXiv preprint arXiv:2503.14476*, 2025.

577 Xiaojiang Zhang, Jinghui Wang, Zifei Cheng, Wenhao Zhuang, Zheng Lin, Minglei Zhang, Shaojie
 578 Wang, Yinghan Cui, Chao Wang, Junyi Peng, et al. Srpo: A cross-domain implementation of
 579 large-scale reinforcement learning on llm. *arXiv preprint arXiv:2504.14286*, 2025.

580 Wayne Xin Zhao, Kun Zhou, Junyi Li, Tianyi Tang, Xiaolei Wang, Yupeng Hou, Yingqian Min,
 581 Beichen Zhang, Junjie Zhang, Zican Dong, et al. A survey of large language models. *arXiv*
 582 *preprint arXiv:2303.18223*, 1(2), 2023.

583 Chujie Zheng, Shixuan Liu, Mingze Li, Xiong-Hui Chen, Bowen Yu, Chang Gao, Kai Dang,
 584 Yuqiong Liu, Rui Men, An Yang, et al. Group sequence policy optimization. *arXiv preprint*
 585 *arXiv:2507.18071*, 2025a.

586 Haizhong Zheng, Rui Liu, Fan Lai, and Atul Prakash. Coverage-centric coreset selection for high
 587 pruning rates. *arXiv preprint arXiv:2210.15809*, 2022.

594 Haizhong Zheng, Yang Zhou, Brian R Bartoldson, Bhavya Kailkhura, Fan Lai, Jiawei Zhao, and
595 Beidi Chen. Act only when it pays: Efficient reinforcement learning for llm reasoning via selective
596 rollouts. *arXiv preprint arXiv:2506.02177*, 2025b.
597
598 Tianyu Zheng, Tianshun Xing, Qingshui Gu, Taoran Liang, Xingwei Qu, Xin Zhou, Yizhi Li, Zhou-
599 futu Wen, Chenghua Lin, Wenhao Huang, et al. First return, entropy-eliciting explore. *arXiv*
600 *preprint arXiv:2507.07017*, 2025c.
601
602 Xiangxin Zhou, Zichen Liu, Anya Sims, Haonan Wang, Tianyu Pang, Chongxuan Li, Liang
603 Wang, Min Lin, and Chao Du. Reinforcing general reasoning without verifiers. *arXiv preprint*
604 *arXiv:2505.21493*, 2025.
605
606
607
608
609
610
611
612
613
614
615
616
617
618
619
620
621
622
623
624
625
626
627
628
629
630
631
632
633
634
635
636
637
638
639
640
641
642
643
644
645
646
647

648

649

650

651

652

653

654

655

656

657

658

659

660

661

662

663

664

665

666

667

668

669

670

671

672

673

674

675

676

677

678

679

680

681

682

683

684

685

686

687

688

689

690

691

692

693

694

695

696

697

698

699

700

701

Appendix

A EXPERIEMNTAL DETAILS

A.1 TRAINING DETAILS

We provide detailed settings of various parameters in the DAPO algorithm, which serves as both the baseline and the optimization method for Reactivated Advantage (RA) and ERPO. The KL coefficient is fixed at 0 across all experiments. The clip ratio is set to $\epsilon_{low} = 0.2$ and $\epsilon_{high} = 0.28$. The maximum response length is set to 10,240 for experiments on the Qwen2.5-3B model and the RA algorithm, and to 20,480 for experiments with DAPO and ERPO on the Qwen2.5-7B model. The overlong buffer is set to 4,096, with an overlong penalty factor of 1. 180 prompt generation steps/2880 policy update steps is used for all emperiments. Experiments with ERPO on Qwen2.5-3B were conducted using $4 \times$ NVIDIA H100 80GB GPUs, while experiments with ERPO on Qwen2.5-7B were conducted using $8 \times$ NVIDIA A100 80GB GPUs.

A.2 EVALUATION DETAILS

We follow the same evaluation protocol as DAPO (Yu et al., 2025), using the verl framework () to assess AIME25, AIME24 and AMC23 benchmarks. Specifically, each question from the benchmark is prepended with the prompt `Solve the following math problem step by step.` The last line of your response should be of the form `Answer: $Answer` (without quotes), where `$Answer` is the solution to the problem.`\n\n` and appended with the prompt `\n\nRemember to put your answer on its own line after "Answer:".` This structure is identical to that used in the training data. We then follow the same workflow as DAPO to extract the final answer from the model responses. For MATH500, we follow Hendrycks et al. (2021) to evaluate the results.

B ADDITIONAL EXPERIMENTAL RESULTS

Comparison with additional baselines. We futher compare our model performance with another baseline Entropy (Cheng et al., 2025), which use the same backbone model Qwen2.5-7B, training dataset DAPO-Math-17K, optimization method DAPO and very similiar hyperparameters. The results are shown in Table 5. Results show that ERPO outperforms Entropy on every benchmark by a large margin, demonstrating the effectiveness of ERPO.

GRPO. To evaluate the effectiveness of ERPO under a different RL algorithm, we compare the performance of vanilla GRPO (Shao et al., 2024) and GRPO+ERPO on Qwen2.5-3B. The training hyperparameters are kept identical to those used in the main experiments. The results are reported in Table 6. These results show that incorporating ERPO leads to consistent improvements across almost all datasets and evaluation metrics. This result further demonstrates the robustness and generality of ERPO, showing that its improvements persist across different RL algorithms.

More Training Steps. To further assess the training stability of ERPO, we train both DAPO and ERPO with 270 prompt-generation steps, corresponding to 4320 policy-update steps on Qwen2.5-3B. The results are shown in Table 7. These findings indicate that ERPO continues to consistently outperform DAPO even under substantially longer training, demonstrating the scalability and robustness of ERPO when compute is increased.

Llama Backbone. To demonstrate the generalize of ERPO under different backbone model, we train Llama-3.2-3B-Instruct with DAPO and ERPO with the same hyperparameters with Qwen2.5-3B. The results are shown in Table 8. ERPO shows consistently improvements over the DAPO baseline using the Llama backbone. This demonstrates that ERPO is not specific to Qwen-series models and can still outperform DAPO under alternative architectures.

Training Performance. We further present the model performance on AIME25 throughout training in Figure 4. On both Qwen2.5-3B and Qwen2.5-7B, ERPO consistently outperforms the DAPO baseline for most of the training process, demonstrating its effectiveness on novel and challenging math tasks that are less affected by data contamination. RA achieves the best performance on

702
 703 Table 5: Performance comparison of the Qwen2.5-7B model trained with the Entropy baseline and
 704 ERPO. For the Entropy baseline, we report the values provided in their paper. For ERPO, we report
 705 the *mean@32* scores on AIME25, AIME24, and AMC23, and the *mean@4* score on MATH500.

Method	AIME25	AIME24	AMC23	MATH500	Avg.
Qwen2.5-7B					
Entropy	11.8	12.6	57.8	58.5	35.2
ERPO	14.2	19.0	76.4	61.7	42.8

711
 712
 713 Table 6: Performance comparison of using the GRPO algorithm with ERPO. Evaluations use
 714 mean@32, maj@32, and pass@32 for AIME25, AIME24, and AMC23; MATH500 is reported
 715 with mean@4, maj@4, and pass@4. The Avg. columns average the mean, maj, and pass across
 716 datasets.

Method	AIME25			AIME24			AMC23			MATH500			Avg.		
	mean@32	maj@32	pass@32	mean@32	maj@32	pass@32	mean@32	maj@32	pass@32	mean@4	maj@4	pass@4	mean	maj	pass
Qwen2.5-3B															
GRPO	2.4	3.1	13.3	6.9	8.1	33.3	44.7	49.5	77.5	31.7	32.9	51.0	21.4	23.4	43.8
+ERPO	4.6	4.2	16.7	7.6	8.6	30.0	50.0	55.8	77.5	35.3	38.1	61.6	24.4	26.7	46.5

721
 722
 723 Table 7: Performance comparison of the Qwen2.5-3B model trained with 270 prompt generation
 724 steps. Evaluations use mean@32, maj@32, and pass@32 for AIME25, AIME24, and AMC23;
 725 MATH500 is reported with mean@4, maj@4, and pass@4. The Avg. columns average the mean,
 726 maj, and pass across datasets.

Method	AIME25			AIME24			AMC23			MATH500			Avg.		
	mean@32	maj@32	pass@32	mean@32	maj@32	pass@32	mean@32	maj@32	pass@32	mean@4	maj@4	pass@4	mean	maj	pass
Qwen2.5-3B															
DAPO	4.2	6.4	23.3	9.6	15.9	26.7	64.2	72.3	82.5	61.2	64.0	76.8	34.8	39.7	52.3
+ERPO	6.4	8.4	33.3	11.1	18.1	26.7	63.9	71.4	85.0	62.2	65.3	78.4	35.9	40.8	55.9

732
 733
 734 Table 8: Performance comparison of the Llama-3.2-3B-Instruct model trained with DAPO, and
 735 +ERPO. Evaluations use mean@32, maj@32, and pass@32 for AIME25, AIME24, and AMC23;
 736 MATH500 is reported with mean@4, maj@4, and pass@4. The Avg. columns average the mean,
 737 maj, and pass across datasets.

Method	AIME25			AIME24			AMC23			MATH500			Avg.		
	mean@32	maj@32	pass@32	mean@32	maj@32	pass@32	mean@32	maj@32	pass@32	mean@4	maj@4	pass@4	mean	maj	pass
Llama-3.2-3B-Instruct															
DAPO	0.6	1.2	6.7	12.3	16.4	30.0	59.1	60.1	70.0	49.4	49.4	63.2	30.4	31.8	42.5
+ERPO	1.1	2.3	6.7	13.9	20.5	30.0	60.9	69.3	75.0	52.5	52.5	67.0	32.1	36.2	44.7

743
 744
 745 Qwen2.5-3B but only the second-best on Qwen2.5-7B, suggesting that training on residual prompts
 746 can provide notable benefits, but its advantages diminish as model size scales up.

747
 748 **Training Entropy.** We report the policy-generation entropy on the training data throughout training
 749 in Figure 5. On Qwen2.5-3B, DAPO exhibits slightly higher entropy than ERPO, whereas on
 750 Qwen2.5-7B, ERPO shows a higher entropy compared to DAPO. In contrast, RA achieves the high-
 751 est entropy on the 3B model but the lowest entropy on the 7B model.

752
 753 **Case Study.** We provide a case study on the Qwen2.5-7B model trained with ERPO, with gener-
 754 ations sampled at temperatures 1.0, 1.2, and 1.4. The detailed examples are shown in Figure 6,
 755 Figure 7, and Figure 8, respectively. Responses produced at different temperatures are all well-
 756 structured and readable. While the model yields the correct final answer at temperature 1.0, the
 757 outputs generated at temperatures 1.2 and 1.4 produce incorrect final answers.

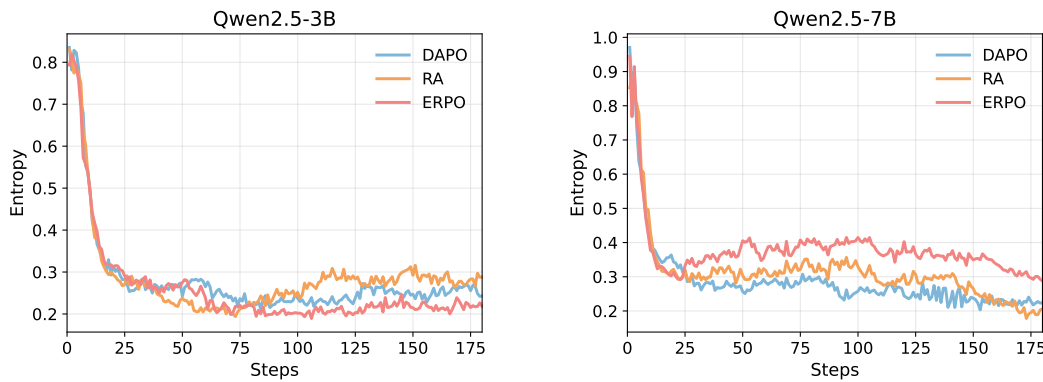
Figure 4: Performance of *mean@32* on AIME2025.

Figure 5: Entropy along training.

USE OF LARGE LANGUAGE MODELS

Large language models were used solely to check grammar and improve the clarity of writing. They were not involved in research ideation, methodology design, data analysis, or experimental results.

810

811

812

813

814

815

916

913

817

818

Sample Temperature: 1.0

Question: Solve the following math problem step by step. The last line of your response should be of the form Answer: \$Answer (without quotes) where \$Answer is the answer to the problem.\n\nTwo towns, \$A\$ and \$B\$, are \$100\$ miles apart. Every \$20\$ minutes (starting at midnight), a bus traveling at \$60\$ mph leaves town \$A\$ for town \$B\$, and every \$30\$ minutes (starting at midnight), a bus traveling at \$20\$ mph leaves town \$B\$ for town \$A\$. Dirk starts in Town \$A\$ and gets on a bus leaving for town \$B\$ at noon. However, Dirk is always afraid he has boarded a bus going in the wrong direction, so each time the bus he is in passes another bus, he gets out and transfers to that other bus. How many hours pass before Dirk finally reaches Town \$B\$?\n\nRemember to put your answer on its own line after "Answer:".

Solution: 5

Response: Let's break down the problem step by step to determine how many hours it will take for Dirk to reach Town B.

Buses from Town A: Buses leave Town A every 20 minutes starting at midnight. Each bus travels at 60 mph.

Buses from Town B: Buses leave Town B every 30 minutes starting at midnight. Each bus travels at 20 mph.

To understand the schedule, let's list the buses departing from Town A and Town B:

Buses from Town A: * Noon: 60 mph bus * 12:20 pm: 60 mph bus * 12:40 pm: 60 mph bus * 1:00 pm: 60 mph bus * 1:20 pm: 60 mph bus * 1:40 pm: 60 mph bus ...

Buses from Town B: * Noon: 20 mph bus * 12:30 pm: 20 mph bus * 1:00 pm: 20 mph bus * 1:30 pm: 20 mph bus * 2:00 pm: 20 mph bus * 2:30 pm: 20 mph bus ...

Given the distance between Town A and Town B is 100 miles, Dirk is in a constant state of transferring as the buses he takes may pass other buses going in the opposite direction.

We need to observe the scenario for Dirk:

At 12:00 PM, Dirk starts on the bus from town A, leaving at 12:00 PM. This bus will travel towards town B at 60 mph.

To determine how many hours it will take for Dirk to reach Town B, we need to follow his bus's schedule and transfers.

Let's determine when each bus from A and B will pass each other:

Buses from A to B: - A bus from A (at $t = 0, 20, 40, 60, \dots$ mph) - A distance of $\frac{60}{60}t = t$ miles (where t is the time in hours since noon).

Buses from B to A: - A bus from B (at $t = 0, 30, 60, 90, \dots$ mph) - A distance of $\frac{20}{60}t = \frac{1}{3}t$ miles (where t is the time in hours since noon).

Now, every time Dirk's bus passes another bus, he gets off and transfers. We need to track these transfers:

Dirk initially starts on the bus that left at noon (60 mph). This bus will reach Town B when it has traveled 100 miles:

$$\frac{60}{60}t = 100$$

$$t = 100$$

However, Dirk will transfer at every point where his bus crosses another bus. We need to calculate these crossings:

Crossing Point Calculations: When a bus from A (speed = 60 mph) and a bus from B (speed = 20 mph) meet, their relative speed is $60 + 20 = 80$ mph.

The distance between the two towns is 100 miles, so the time to meet is $\frac{100}{80} = 1.25$ hours.

Buses Leaving at the Same Time: Let's consider a bus from A that leaves at time t_1 and a bus from B that leaves at time t_2 .

The position of the A bus at time t is $60(t - t_1)$.

The position of the B bus at time t is $20(t - t_2)$.

When these buses meet, their positions equal:

$$60(t - t_1) = 20(t - t_2)$$

$$40t - 40t_1 = 20t - 20t_2$$

$$20t = 40t_1 - 20t_2$$

$$t = \frac{40t_1 - 20t_2}{20}$$

Simplifying this, we get:

$$t = 2t_1 - t_2$$

To make this easier, let's look for a pattern in the transfers:

Initially, Dirk is on a bus that left at 12:00 PM. This bus will pass another bus every 1.25 hours. Dirk will transfer at these times:

1. First transfer: The bus from A that left at 12:20 (20 minutes later) will meet the bus of interest which left at 12:00.

2. Second transfer: When Dirk's initial bus passes another bus, he will transfer, and so on.

To simplify, we need to consider the bus schedules:

Dirk will transfer at every 1.25-hour interval:

At $t = 1.25, 2.5, 3.75, \dots$ hours, etc.

To reach Town B, we need to determine when Dirk finally reaches it without further transfers.

Let's calculate:

If Dirk stays on his initial bus, the time to reach B is $\frac{100}{60} = \frac{5}{3} \approx 1.67$ hours.

However, we need to consider the transfers. Dirk will transfer every 1.25 hours. Let's calculate when he finally reaches Town B without further transfers.

Dirk will transfer at these times until he finally reaches Town B. We need to determine when he reaches Town B without further transfers.

Dirk will transfer multiple times, but since the problem asks for when he finally reaches Town B, we need the first time he reaches it without further transferring.

The time taken for Dirk to reach Town B, without further transfers, will be when he reaches Town B directly. The time to reach B directly is $\frac{100}{60} = \frac{5}{3} \approx 1.67$ hours. However, we need to consider the transfers as well.

To find the exact time, we need to consider the following:

1. Dirk will transfer at every 1.25 hours.

2. We need to calculate the time when he finally reaches Town B.

The time when Dirk finally reaches Town B without further transfers will be when he crosses the last bus from B. Let's calculate:

Dirk needs 1.67 hours to reach Town B directly. However, since he will transfer every 1.25 hours, we need to find the exact time.

Answer: 5

Figure 6: Case study on the Qwen2.5-7B model trained with ERPO, with generations sampled at temperature 1.0.

864
865
866
867
868
869
870
871
872

Sample Temperature: 1.2

873 **Question:** Solve the following math problem step by step. The last line of your response should be of the form
874 Answer: \$Answer (without quotes) where \$Answer is the answer to the problem.\n\nTwo towns, \$A\$ and
875 \$B\$, are \$100\$ miles apart. Every \$20\$ minutes (starting at midnight), a bus traveling at \$60\$ mph leaves town
876 \$A\$ for town \$B\$, and every \$30\$ minutes (starting at midnight), a bus traveling at \$20\$ mph leaves town \$B\$
877 for town \$A\$. Dirk starts in Town \$A\$ and gets on a bus leaving for town \$B\$ at noon. However, Dirk is always
878 afraid he has boarded a bus going in the wrong direction, so each time the bus he is in passes another bus, he
879 gets out and transfers to that other bus. How many hours pass before Dirk finally reaches Town
880 \$B\$?\n\nRemember to put your answer on its own line after "Answer:".

881 **Solution:** 5

882 **Response:** In order to solve the problem step by step, let us break it down by finding the intervals and locations
883 of the buses as they are relevant to Dirk and his movements. Dirk starts in Town A at noon and gets on a bus at
884 that time. Let us calculate the schedule for the buses leaving from both A and B.\n\n1. Buses Leaving from A:
885 These buses leave A every 20 minutes (0, 20, 40, 60, 80... minutes), and they all travel at 60 mph from A to B,
886 100 miles apart.\n\n2. Buses Leaving from B: These buses leave B every 30 minutes (0, 30, 60, 90... minutes), and
887 they travel at 20 mph from B to A, 100 miles apart.\n\nLet's calculate some times when buses pass each other,
888 as Dirk will transfer to a bus if a bus from the opposite town passes his. We will determine where a bus from A
889 meets a bus from B to help us track Dirk's movement.\n\nLet t be the time passed in hours since
890 midnight.\n\n**Buses Leaving from A:**\nThese buses depart at:\n- 0 (12:00 AM)\n- 20/60 (0.3333 hours or
891 20 minutes)\n- 40/60 (0.6667 hours or 40 minutes)\n- 60/60 (1 hour)\n- 80/60 (1.3333 hours or 80
892 minutes)\n\nTheir position in Miles after Δt hours is given by:\n $A_{bu} = 60t$ (since they travel from A to
893 B, 100 miles).\n\n**Buses Leaving from B:**\nThese buses depart at:\n- 0 (12:00 AM)\n- 30/60 (0.5 hours or
894 30 minutes)\n- 1 (1 hour)\n- 1.5 (1.5 hours or 90 minutes)\n\nTheir position when they reach A is given
895 by: $B_{bu} = 20t$ (since they travel from B to A, 100 miles).\n\n### First Transfer Point:\nTo determine if
896 there will be any transfers, let's check when a bus leaves from A will pass a bus leaving from B.\n\nThe position
897 of an A bus after Δt hours will meet a B bus, which started at time $t - \Delta t$, where Δt is in hours. Let us calculate the crossing of an A and B bus.\n\nThe bus that departs A at 0 (12:00 AM) at t hours will meet a B bus leaving A at $t - \Delta t$ hours at position $60t = 20(t - \Delta t)$. This will occur where these positions are equal.\n\nSimplify:
 $60t = 20(t - \Delta t)$
 $60t = 20t - 20\Delta t$
 $40t = -20\Delta t$
Therefore, $\Delta t = -2t$. This means a bus from town A is never passing a bus from town B since the equation doesn't make sense as $t < 0$ which cannot be positive.\n\nHowever, a more useful approach is to calculate when a bus leaving A at 0 (12:00 AM) will pass a bus leaving B. Let us calculate the passing times step by step.\n\nA bus departing A at 0 (12:00 AM) will pass a bus from B which departed B a $t/3$ hours ago (as the second bus from B departs every 30 minutes).\n\nLet's calculate when buses leaving A at 0 and B and compare:\n- First bus A at 0 leaves at 0 hours, B at 0 from B leaves at 0 hours.\n- Second bus A at 20 minutes (0.3333 hours) and the B bus from that time will leave at $30/60 = 0.5$ hours.\n\nTo find when this happens, let's consider some calculations based on the times of arrival.\nAt t hours, an A bus will have traveled $60t$ miles and a B bus will have traveled $20t$ miles.\n\nTo find the meeting points:\n\nCalculate when an A bus at, and a B bus at the same location:\n- The two buses (A and B) will meet when: $60t = 100 - 20(t - \Delta t)$ where Δt is an integer multiple of $20/60$ and $t - \Delta t$ is an integer multiple of $30/60$.

900 **Answer:** 3.212 hours\nHence, 3.212 hours is before
901 Dirk reaches Town B. We need to figure out when Dirk finally reaches Town B.\n\n**Answer:** 6",

902
903
904
905
906
907
908
909
910
911
912
913
914
915
916
917

